Quantum Electronics **48** (10) 886–893 (2018)

https://doi.org/10.1070/QEL16765

Three-photon laser excitation of mesoscopic ensembles of cold rubidium Rydberg atoms

E.A. Yakshina, D.B. Tretyakov, V.M. Entin, I.I. Beterov, I.I. Ryabtsev

Abstract. **The spectra of three-photon laser excitation (according to the $^5S_{1/2} \rightarrow {}^5P_{3/2} \rightarrow {}^6S_{1/2} \rightarrow {}^{37}P_{3/2}$ scheme) of mesoscopic ensembles of cold Rb Rydberg atoms in a magneto-optical trap, using cw single-frequency lasers in each stage, have been investigated. The ensembles consisted of 1 to 5 atoms, and their presence was recorded by the selective field ionisation method with postselection according to the number of atoms. The dependence of the spectral shape on the excitation laser pulse duration has been studied. For 2-μs pulses, the minimum spectral width was found to be 1.3 MHz; it was determined by the laser linewidth and the spectral width of laser pulse. For pulses shorter than 0.5 μs, additional spectral broadening and occurrence of Rabi oscillations in the wings of three-photon resonances have been observed, a fact indicative of implementation of coherent three-photon laser excitation of Rydberg atoms. An analysis of the spectra within the four-level theoretical model based on optical Bloch equations showed good agreement between the experimental and theoretical results. The dependence of the shape of three-photon excitation spectrum on the number of recorded atoms was also studied. An increase in the average number of atoms leads to the occurrence of a dip in the single-atom excitation spectra; this dip is due to the specificity of the excitation and detection statistics of Rydberg atoms. The results obtained are important for applications of Rydberg atoms in quantum informatics.**

Keywords: *Rydberg atoms, three-photon excitation, spectroscopy, detection statistics, laser cooling.*

1. Introduction

Rydberg atoms with the principal quantum number $n \gg 1$ are unique objects for high-resolution spectroscopy and quantum electrodynamics experiments due to their long lifetime, transition frequencies lying in the IR and microwave spectral regions, transition dipole moments on the order of several thousand atomic units or more, and high sensitivity to external electromagnetic fields [1]. Exact theoretical models of interaction with an electromagnetic field can be developed for a weakly bound electron in a Rydberg atom, with subsequent comparison of simulation data with experimental results.

A unique feature of Rydberg atoms is the possibility of detecting them by the selective field ionisation (SFI) method using a weak electric field (an electric field with a strength exceeding some critical value, determined by the quantum numbers nL, ionises the atom with a probability close to 1); in this case, single atoms can be detected with an electron multiplier [2]. This method allows one to determine both the total number of Rydberg atoms and the relative populations of different Rydberg states. Thus, experiments with one or several atoms can be performed.

The aforementioned properties make it possible to use atoms in Rydberg states for new urgent studies in the field of atomic and quantum physics, during which the states of individual quantum particles must be controlled and monitored. Laser excitation of Rydberg atoms with a high spectral resolution is necessary in the experiments aimed at studying the potential of these atoms in a number of urgent applications, such as quantum information processing [3–6] or phase transitions in cold ensembles of interacting Rydberg atoms [7, 8].

Experiments with cold Rb Rydberg atoms are generally performed applying the two-step excitation scheme 5S → 5P → nS, nD for the Rydberg nS and nD states from the ground state 5S through the intermediate state 5P using radiation with wavelengths of 780 and 480 nm [4, 6, 9, 10]. Similar two-step schemes are used for laser excitation of other Rydberg atoms [11–13].

An interesting feature of the three-photon laser excitation is that one can excite cold Rydberg atoms without the recoil and Doppler effects, thus excluding heating of the atoms as a result of photon absorption and providing a high accuracy of quantum operations with Rydberg atoms. It was previously shown by us in the theoretical study [14] that a necessary condition for this excitation is the equality of the sum of the wave vectors of excitation laser beams to zero. The one-step (5S → nP) and two-step (5S → 5P → nS,nD) excitation schemes for Rb atoms do not satisfy this condition. However, one can implement a three-step scheme (5S → 5P → 6S → nP) by directing three laser beams to an ensemble of cold atoms from three different sides under certain angles relative to each other. The intermediate resonances of this transition should have large detunings to exclude population of short-lived intermediate levels. In this case, the calculated excitation spectra of Rydberg states exhibit narrow Doppler-free resonances with a width determined by only the interaction time of atoms with laser radiation; this holds true for

E.A. Yakshina, D.B. Tretyakov, V.M. Entin, I.I. Ryabtsev
A.V. Rzhanov Institute of Semiconductor Physics, Siberian Branch, Russian Academy of Sciences, prosp. Akad. Lavrent'eva 13, 630090 Novosibirsk, Russia; Novosibirsk State University, ul. Pirogova 2, Novosibirsk, 630090 Russia; e-mail: ryabtsev@isp.nsc.ru;
I.I. Beterov A.V. Rzhanov Institute of Semiconductor Physics, Siberian Branch, Russian Academy of Sciences, prosp. Akad. Lavrent'eva 13, 630090 Novosibirsk, Russia; Novosibirsk State University, ul. Pirogova 2, 630090 Novosibirsk, Russia; Novosibirsk State Technical University, prosp. Karla Marksa 20, 630073 Novosibirsk, Russia

Received 11 June 2018; revision received 20 July 2018
Kvantovaya Elektronika **48** (10) 886–893 (2018)
Translated by Yu.P. Sin'kov

both ultracold and hot (room-temperature) atoms. However, this star-shaped geometry of three-photon laser excitation has not been implemented yet, because it calls for the development of a special magneto-optical trap (MOT) with a certain configuration of the optical windows in its vacuum chamber.

In this paper, we report the results of experimental and theoretical study of the spectra of three-photon laser excitation (according to the $5S_{1/2} \rightarrow 5P_{3/2} \rightarrow 6S_{1/2} \rightarrow 37P_{3/2}$ scheme) of mesoscopic ensembles of cold Rb Rydberg atoms in a MOT, using cw single-frequency lasers in each stage. The ensembles consisted of $N = 1-5$ atoms and were recorded by the SFI method, with postselection according to the number of atoms. The dependence of the excitation spectrum shape on the duration of the excitation laser pulse and the number of recorded Rydberg atoms was analysed.

2. Experimental setup

Experiments were performed with cold ^{85}Rb atoms captured in an MOT, which is schematically shown in Fig. 1a [5, 15]. Atoms are cooled by three orthogonally propagating pairs of light waves with a wavelength of 780 nm. The cooling laser radiation was tuned to the closed transition $5S_{1/2}(F=3) \rightarrow 5P_{3/2}(F=4)$ in the ^{85}Rb isotope, and the transfer laser radiation was tuned to the $5S_{1/2}(F=2) \rightarrow 5P_{3/2}(F=3)$ transition. A cloud consisting of $\sim 10^6$ cold atoms with a size of 0.5–1 mm, cooled to 100–200 μK, is formed in the trap centre.

Cold Rb atoms are excited to the Rydberg states nP (n = 30–100) according to the three-stage scheme: $5S_{1/2} \rightarrow 5P_{3/2} \rightarrow 6S_{1/2} \rightarrow 37P_{3/2}$ (Fig. 1b). In the first stage, the ($5S_{1/2}(F=3) \rightarrow 5P_{3/2}(F=4)$) transition is excited by a cw external-cavity semiconductor Toptica DL PRO laser with a radiation wavelength λ = 780 nm and output power up to 50 mW. The laser is equipped with a built-in Faraday isolator and a fibre output. The laser frequency is stabilised by the Pound–Drever–Hall method with respect to the saturated-absorption resonance in a cell with Rb vapour. The width of the $\Gamma_1/(2\pi)$ lasing line was measured to be ~0.3 MHz. The laser output radiation is transmitted through an acousto-optic modulator (AOM), which forms pulses of specified duration with 100-ns fronts. This AOM also provides a blue detuning $\delta_1/(2\pi)$ = +80 MHz

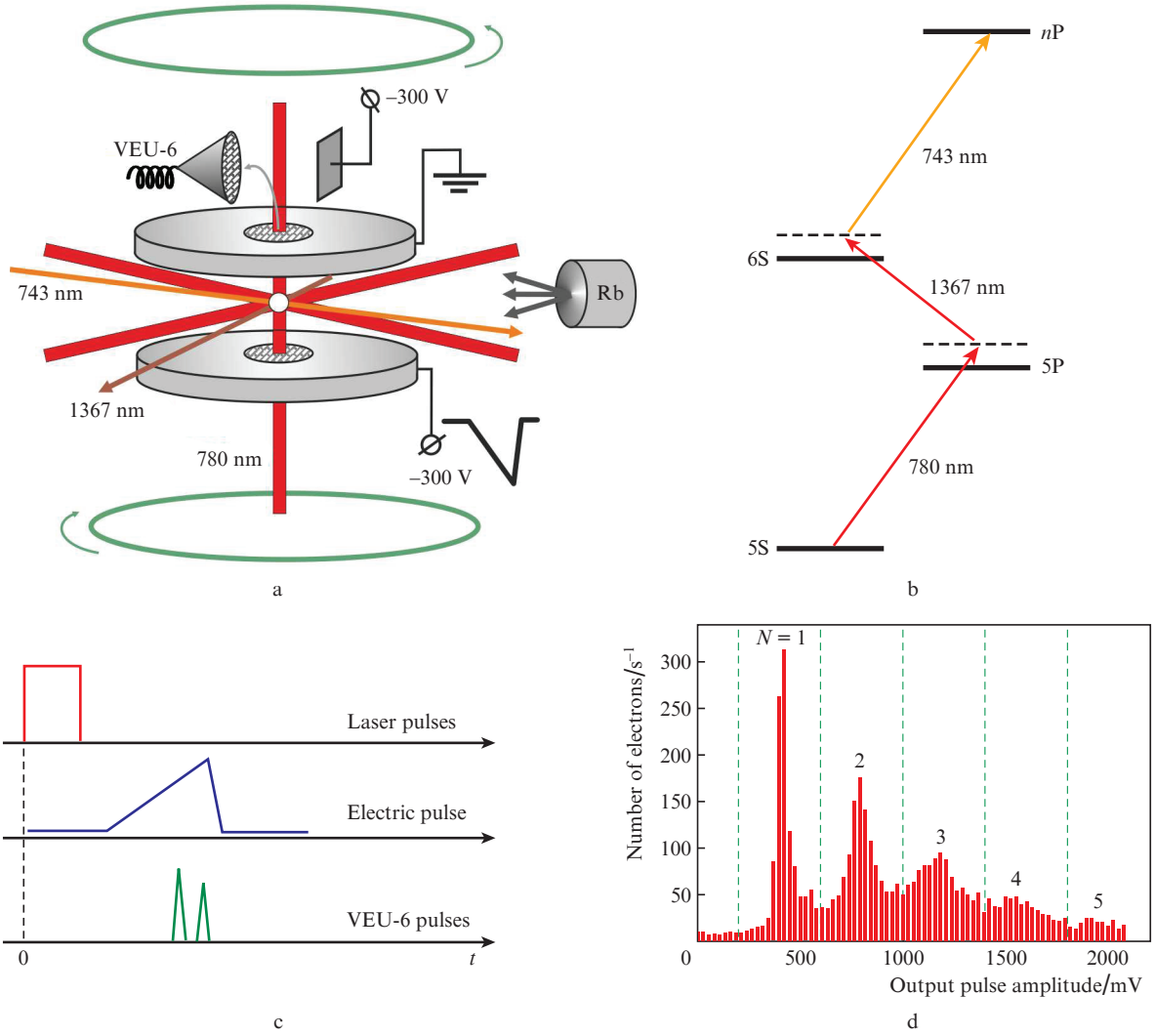

Figure 1. (a) Schematic of the experiment with cold ^{85}Rb Rydberg atoms in a MOT; (b) schematic of coherent three-photon laser excitation $5S_{1/2} \rightarrow 5P_{3/2} \rightarrow 6S_{1/2} \rightarrow n$P of Rb Rydberg atoms, with detuning from intermediate resonances; (c) time diagram of laser and electric pulses; and (d) histogram of the output pulses of the VEU-6 multiplier, which detects electrons formed as a result of SFI.

from the exact atomic resonance in order to prevent the intermediate level $^5P_{3/2}$ from occupation.

In the second stage ($5P_{3/2}(F=4) \rightarrow 6S_{1/2}(F=3)$), radiation of a cw single-frequency external-cavity semiconductor Sacher TEC150 laser (λ = 1367 nm) with a built-in Faraday isolator and a fibre output with an output power up to 30 mW is used. The laser radiation frequency is stabilised by the Pound–Drever–Hall method with respect to the resonance of a highly stable optical Fabry–Perot Stable Laser Systems ATF interferometer. The linewidth $\Gamma_2/(2\pi)$ was measured to be ~0.3 MHz. The output laser radiation is transmitted through an electro-optic modulator (EOM) with a modulation depth of 20 dB, which forms pulses of specified duration with 2-ns fronts. The radiation frequency also has a blue detuning $\delta_2/(2\pi)$ = +82 MHz from the exact atomic resonance to exclude occupation of the intermediate level $6S_{1/2}$.

In the third stage, Rydberg nP states are excited from the $6S_{1/2}(F=3)$ state by radiation of a cw ring Ti:sapphire Tekhnoscan TIS-SF-07 laser with an output power up to 500 mW. Tuning the radiation wavelength in the range from 738 to 745 nm, one can selectively excite fine-structure sublevels with J = 1/2, 3/2 of the Rydberg nP states having principal quantum numbers n = 30–120. The radiation frequency is stabilised by the Pound–Drever–Hall method with respect to the resonance of the same highly stable optical Fabry–Perot Stable Laser Systems ATF interferometer. The measured linewidth $\Gamma_3/(2\pi)$ is ~0.01 MHz. An AOM is installed at the laser output to generate pulses with 100-ns fronts.

The second- and third-stage laser beams are supplied to the MOT through single-mode optical fibres. The beams are collimated at the fibre outputs and then focused to a cloud of cold atoms in the orthogonal-beam geometry (Fig. 1a), with waist diameters of 10 and 20 μm for the beams with λ = 743 and 1367 nm, respectively. An ensemble of excited Rydberg atoms with an effective size of 20–50 μm, depending on the mutual position of the beam waists and the presence (or absence) of transition saturation, is formed in the focused-beam intersection region. The first-stage laser beam (λ = 780 nm), which is 1 mm in diameter, is not focused. It is directed to the cloud of cold atoms at angles of 45° with respect to the other beams. Rydberg atoms are excited by laser pulses with a repetition rate of 5 kHz.

Rydberg atoms are excited in the gap between two stainless steel plates, which form a uniform electric field (Fig. 1a). This electric field is used for Stark spectroscopy and detection of Rydberg atoms by the SFI method [1]. Rydberg atoms are detected at a pulse repetition rate of 5 kHz, with an ionising electric field sweep pulse (having a rise time of 2–3 μs) switched on. The electrons formed as a result of the ionisation are accelerated by the electric field, pass through the metal mesh of the upper plate, and are directed (using a deflection electrode) to the input aperture of a channel-type electron VEU-6 multiplier. Pulsed signals from the multiplier output are processed using a high-speed ADC, a strobe integrator, and a computer. The number of electrons detected per laser pulse is determined by the number of Rydberg atoms in the excitation region and the total electron detection efficiency [2]. The detection efficiency reached 70% in our experiments [16, 17].

The time diagram of signals in the detection system is shown in Fig. 1c. After each laser pulse, exciting some part of cold atoms to the Rydberg state nP, the ionising electric field sweep pulse with a rise time of about 2 μs was switched on. Depending on the Rydberg atom state, ionisation occurred at different instants after the laser pulse. Then an ionisation signal pulse was recorded at the VEU-6 output using a strobe pulse with a duration corresponding to the nP-state ionisation time. A histogram of VEU-6 output pulse amplitudes is shown in Fig. 1d. One can see several peaks, corresponding to different numbers of detected Rydberg atoms N = 1–5. The integral amplitude (area) of each peak is described by the Poisson distribution and depends on the average number of detected atoms per laser pulse. In Fig. 1d, this value is 2.2 atoms per pulse; the probabilities of one- and two-atom excitation are approximately equal, but the one-atom peak is narrower and higher. The statistical data on the laser excitation and detection of Rydberg atoms are discussed in more detail in Section 5 [see formulae (3)–(7)].

After each laser pulse, the acquisition data system measured the VEU-6 output pulse amplitude and then determined (using the previously obtained histogram, Fig. 1d) the number of detected atoms. When data for 10^3–10^4 laser pulses were accumulated, this system sorted signals with respect to the number of atoms N and calculated the probability of three-photon laser excitation of Rydberg state. The number of atoms was determined according to the interval of VEU-6 output pulse voltages into which a specific measured signal fell; for example, one atom corresponded to a range of 200–600 mV, two atoms corresponded by a range 600–1000 mV, three atoms corresponded to a range of 1000–1400 mV, etc. The relevant detection thresholds are indicated by vertical dashed lines in Fig. 1d.

Experiments on three-photon excitation spectroscopy were performed in a MOT, previously switched off for a short time. To this end, AOMs were inserted in all cooling laser beams to switch them off for 20 μs and then (after the measurement) switch on again. The MOT gradient magnetic field was not switched off during measurements; however, its influence was minimised by placing the excitation region to the point with a zero magnetic field. The procedure was controlled by the absence of Zeeman splitting of the microwave transition $37P_{3/2} \rightarrow 37S_{1/2}$ at a frequency of 80 GHz, according to the method proposed by us in [18]. This approach made it possible to use a high repetition rate of laser pulses (5 kHz) and perform real-time tracking of changes in the signals from Rydberg atoms on an oscilloscope screen and in the computer-based data acquisition system.

3. Theoretical description of three-photon laser excitation

Let us enumerate the ground state $5S_{1/2}(F=3)$, the first intermediate state $5P_{3/2}(F=4)$, the second intermediate state $6S_{1/2}(F=3)$, and the Rydberg state $nP_{3/2}$ as 1, 2, 3, and 4, respectively (Fig. 1b), and introduce the corresponding Rabi frequency $\Omega_j = d_j E_j/\hbar$ (d_j are dipole moments of single-photon transitions, E_j are the electric field amplitudes for linearly polarised light fields) and detuning δ_j for each intermediate single-photon transition with a number j = 1, 2, or 3. Scanning of the total detuning $\delta = \delta_1 + \delta_2 + \delta_3$ of the three-photon transition $0 \rightarrow 3$ can be performed by scanning the detuning of any transition.

As was shown by us in [14], in the absence of spontaneous relaxation of all levels and at sufficiently large detunings of intermediate resonances ($\Omega_1 \ll |\delta_1|$, $\Omega_2 \ll |\delta_2|$), the Rydberg state population can be calculated by solving the

Schrödinger equation in order to determine the amplitude probabilities a_j for excitation of each level ($j = 0-3$) in the rotating-wave approximation. As a result, one obtains the following dependence of the Rydberg state population on the interaction time t upon coherent three-step (or three-photon) laser excitation:

$$|a_3|^2 \approx \frac{\Omega^2}{\Omega^2 + (\delta + \Delta_0 + \Delta_3)^2}$$

$$\times\{1 - \cos[t\sqrt{\Omega^2 + (\delta + \Delta_0 + \Delta_3)^2}]\}/2, \qquad (1)$$

where $\Omega = \Omega_1\Omega_2\Omega_3/(4\delta_1\delta_3)$ is the effective Rabi frequency upon three-photon excitation and $\Delta_0 = \Omega_1^2/(4\delta_1)$ and $\Delta_3 = \Omega_3^2/(4\delta_3)$ are, respectively, the light shifts of states 0 and 3. Equation (1) shows that the condition for exact three-photon resonance is the equality $\delta + \Delta = 0$, where the complete light shift is $\Delta = \Delta_0 + \Delta_3$; the population oscillates between the ground and Rydberg states at the frequency Ω. This equation describes also the excitation spectrum of the Rydberg state when δ is scanned, while the interaction time t is fixed.

In the more realistic theoretical model, which takes into account the spontaneous relaxation of excited levels 1–3, Rabi oscillations decay with a constant $\gamma = 1/\tau$ (determined by the inverse lifetime τ of Rydberg state) or even more rapidly if the detuning from the intermediate resonances is insufficiently large. Under these conditions, the Rydberg state population tends to some constant value. This model was constructed by us in the four-level approximation based on the optical Bloch equations for the density matrix [15]. Since an exact analytical solution cannot be found for the Rydberg state population ρ_{33} at arbitrary Rabi frequencies and detunings, the problem must be solved numerically in the general case. However, in the case of weak excitation ($\Omega \ll \gamma$), we found the following approximate analytical solution:

$$|a_3|^2 = \rho_{33} \approx \frac{\Omega^2}{2\Omega^2 + \gamma^2 + 4\delta^2}$$

$$\times[1 + \exp(-\gamma t) - 2\exp(-\gamma t/2)\cos(t\sqrt{\Omega^2 + \delta^2})]. \qquad (2)$$

It follows from this solution that, for long interaction times ($\gamma t \gg 1$), Rabi oscillations decay, and the population tends to a constant value, described by the Lorentzian profile of the excitation spectrum.

In addition, the developed theoretical model [15] allows one to take into account the finite linewidths Γ_j of all three laser beams in the phase-diffusion model, when the random phase fluctuations are present in the laser radiation but amplitude fluctuations are absent [19]. To this end, an imaginary part (equal to $\Gamma_j/2$ in modulus) was introduced into each detuning δ_j in the equations for optical coherences in order to provide additional damping for coherence. Our numerical calculations within this model showed good agreement between the experimental and theoretical results [15]. However, it should be noted that the lasing spectrum has a Lorentzian shape in this model, whereas it is generally characterised by a Gaussian profile with a sharper decrease in the wings. Therefore, the theoretical excitation spectra for Rydberg states in the aforementioned model may somewhat differ from the experimental data obtained in the resonance wings.

4. Laser excitation spectra of the three-photon transition $5S_{1/2} \rightarrow 5P_{3/2} \rightarrow 6S_{1/2} \rightarrow 37P_{3/2}$

The excitation spectrum of the Rydberg state $^{37}P_{3/2}$ of Rb atoms is most interesting for us, because the electrically controlled Förster resonances between two [16] or three [17] Rydberg atoms were observed for the first time specifically in this state. Figure 2 shows the experimental spectra of three-photon laser excitation of this state, recorded when scanning the detuning δ_3 for different interaction times t, three-photon Rabi frequencies Ω, and dynamic light shifts Δ, as well as the results of numerical calculations within the four-level theoretical model proposed in [15]. In all cases the theory is in good agreement with experiment. Based on the analysis of the presented spectra, the following conclusions can be drawn.

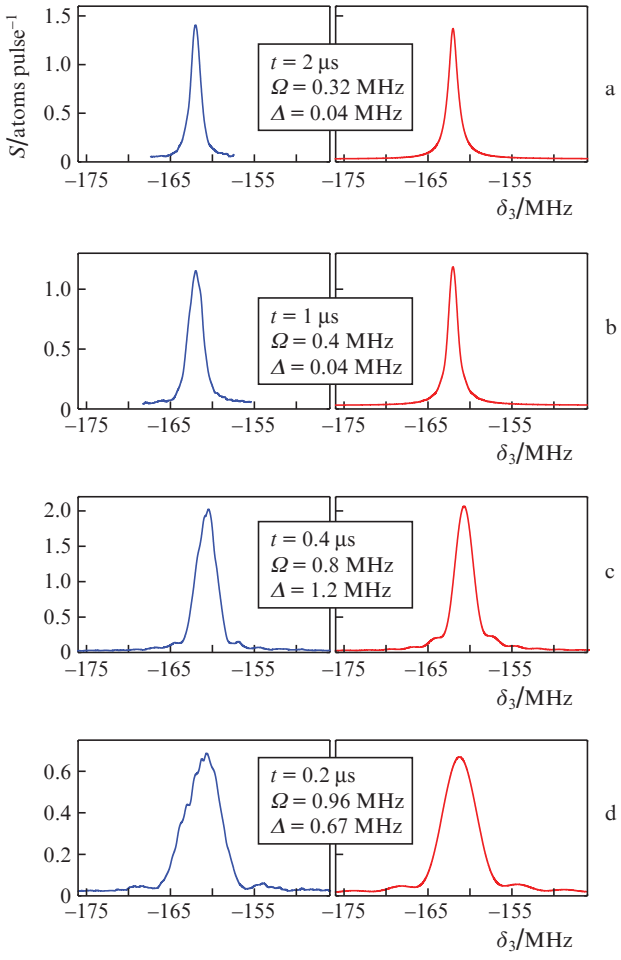

Figure 2. Experimental spectra S of three-photon laser excitation of the Rydberg state $^{37}P_{3/2}$ upon scanning the detuning δ_3 for different interaction times t, three-photon Rabi frequencies Ω, and dynamic light shifts Δ (left column) and the results of numerical calculations according to the four-level model [15] (right column).

First, the three-photon resonance occurs at the detuning $\delta_3 \approx -162$ MHz, which is a consequence of the total detuning $\delta_1 + \delta_2 = +162$ MHz from the two intermediate resonances. This resonance corresponds to the coherent three-photon excitation without occupation of the intermediate levels $5P_{3/2}$

and $6S_{1/2}$, in contrast to the incoherent three-step resonance at $\delta_3 = 0$, when the $5P_{3/2}$ and $6S_{1/2}$ states are partially occupied on the wings of the Lorentzian absorption profiles in the first and second excitation stages. The differences between these processes were discussed by us in [15]. In particular, the coherent three-photon excitation corresponds to simultaneous absorption of all three photons, whereas upon three-stage excitation photons can be absorbed at different instants, which leads to dephasing and coherence loss. Specifically for this reason Rabi oscillations are observed only in the case of coherent three-photon laser excitation. It can be seen in Fig. 2 that an increase in the Rabi frequency Ω leads also to an increase in the dynamic shift Δ of three-photon resonances; however, this shift is relatively small and coincides with Ω in order of magnitude.

Second, the minimum width of the three-photon resonance (1.3 MHz) is observed at the maximum (2 μs) interaction time (Fig. 2a) for a relatively small value of $\Omega/(2\pi) \approx 0.3$ MHz. Here, the resonance width is due to the total linewidth of the three laser beams, $(\Gamma_1 + \Gamma_2 + \Gamma_3)/(2\pi) \approx 0.6$ MHz; the dynamic power broadening $\Omega/(2\pi) \approx 0.3$ MHz; and the spectral width of the excitation laser pulse, $1/t \approx 0.5$ MHz. As follows from Eqns (1) and (2), the latter two factors do not affect the coherence, whereas the nonzero width of lasing lines stipulates the relatively low coherence time of laser pulse $[1/(\Gamma_1 + \Gamma_2 + \Gamma_3) \approx 0.3$ μs] and does not make it possible to observe Rabi oscillations in the spectrum, predicted by Eqns (1) and (2) for the excitation time of 2 μs (Fig. 2a). The same holds true for the spectrum corresponding to the excitation time of 1 μs (Fig. 2b).

Third, with a further decrease in the interaction time to 0.4 μs (Fig. 2c), signs of the structure described by formula (2) and corresponding to Rabi oscillations arise in the spectrum on the resonance wings; the incomplete contrast of this structure indicates the presence of dephasing and only partial coherence of oscillations. However, a decrease in the interaction time to 0.2 μs provides a spectrum with a fairly contrast Rabi oscillation pattern in the resonance wings (Fig. 2d), a fact indicative of achievement of coherent three-photon laser excitation of Rydberg atoms. Based on the data in the literature, we can state that this excitation has been implemented for the first time. At the same time, a decrease in the laser pulse duration broadens the resonances to 2.4 MHz for the spectrum presented in Fig. 2c and to 3.8 MHz for the spectrum in Fig. 2d.

Fourth, the obtained minimum width of three-photon resonances (1.3 MHz) is much smaller than the values (more than 5 MHz) obtained by us in previous experiments [5, 15]. This is a consequence of our efforts to stabilise frequencies and narrow linewidths by locking them (using the Pound–Drever–Hall method) to saturated-absorption resonances or resonances of a highly stable Fabry–Perot interferometer. However, idealally, to perform quantum gates with Rydberg atoms [6], one should increase the coherence time to 100 μs or even more; correspondingly, the linewidths must be narrowed even more to 1 kHz or less. To this end, it is necessary to upgrade the frequency stabilisation system and increase the feedback bandwidth. In addition, to reduce the influence of the residual Doppler effect, it is reasonable to implement three-photon laser excitation without recoil and Doppler effects based on the star-shaped geometry of three laser beams, provided that the sum of their wave vectors is equal to zero, as was proposed by us in [14].

5. Three-photon laser excitation of mesoscopic ensembles of cold Rydberg atoms

Since the SFI-based system for detecting Rydberg atoms that was used in this study makes it possible to measure the number of atoms N and perform postselection of signals with their sorting according to the N value, we analysed the spectra of three-photon laser excitation of mesoscopic ensembles of cold Rydberg atoms with $N = 1-5$.

Figure 3 shows the experimental spectra of three-photon laser excitation of the Rydberg state $37P_{3/2}$ for different Rabi frequencies Ω at the interaction time $t = 2$ μs. The S_1-S_5 notation is used for the excitation spectra of mesoscopic ensembles with a certain number of Rydberg atoms ($N = 1-5$), and the S value, equal to their sum, is a signal corresponding to the average number of Rydberg atoms detected per laser pulse.

The spectra of total signal S exhibit both an increase in the amplitude of three-photon resonance and its width with an increase in Ω, in correspondence with Eqns (1) and (5) (see below). These spectra are described well numerically within our four-level theoretical model.

An essentially new result of our study is that excitation spectra of mesoscopic ensembles S_N were recorded for different N. This feature of our experimental setup was demonstrated for the first time in [3] by an example of microwave transitions between Rydberg states. In the absence of interatomic interactions, these spectra are described by the excitation and detection statistics of Rydberg atoms [2].

Let the excitation volume contain a mesoscopic ensemble of N_0 Rb atoms in the ground state before the laser pulse arrival. During the laser pulse, there is a nonzero probability p of excitation of each atom to the Rydberg state; this probability depends on the three-photon detuning and is described (under certain conditions) by Eqn (1) or (2). Then the average number of Rydberg atoms excited per pulse is

$$\bar{N} = pN_0. \tag{3}$$

The statistics of the number of Rydberg atoms excited per laser pulse depends on p. Upon weak excitation ($p \ll 1$) one can describe the probability P_N^{weak} of detecting N Rydberg atoms after one laser pulse by the Poisson distribution:

$$P_N^{\text{weak}} = \frac{(\bar{N})^N}{N!}\exp(-\bar{N}). \tag{4}$$

However, in the general case, including strong coherent excitation with Rabi oscillations, one should use the more complex normal distribution

$$P_N^{\text{strong}} = p^N(1-p)^{N_0-N}\frac{N_0!}{N!(N_0-N)!}, \tag{5}$$

which is valid for any p and N_0. Specifically this statistical distribution would be observed for an ideal detector of Rydberg atoms with a detection probability $T = 1$.

The detection probability for real detectors is always smaller than unity. For example, the detection probability in our experiments [16, 17] was found to be about 0.7, which is a record value for Rydberg atoms. It can easily be shown that, with allowance for the finite detection probability, the

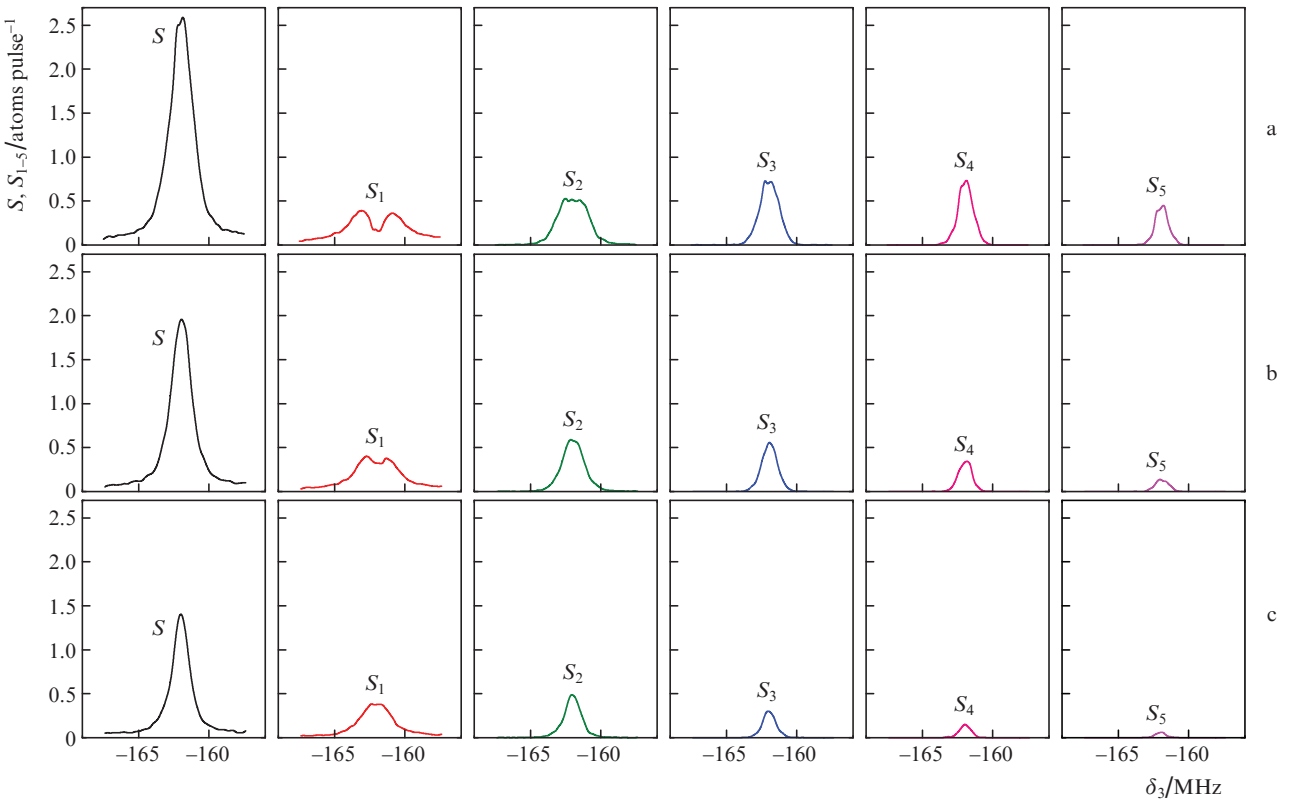

Figure 3. Experimental spectra of three-photon laser excitation of the Rydberg state $^{37}P_{3/2}$ for the Rabi frequencies Ω = (a) 0.43, (b) 0.38, and (c) 0.28 MHz and interaction time $t = 2$ μs: signal S, corresponding to the average number of Rydberg atoms detected per laser pulse, and signals S_1–S_5, which are excitation spectra of mesoscopic ensembles with a certain number of Rydberg atoms: $N = 1$–5.

following distributions are valid for the probability of detecting N Rydberg atoms:

$$\bar{P}_N^{\text{weak}} = \frac{(\bar{N}T)^N}{N!}\exp(-\bar{N}T), \tag{6}$$

$$\bar{P}_N^{\text{strong}} = (pT)^N(1-pT)^{N_0-N}\frac{N_0!}{N!(N_0-N)!}. \tag{7}$$

Thus, the average number of Rydberg atoms detected per laser pulse decreases to $\bar{N}T$. Specifically this value is measured in experiments when averaging over a large number of laser pulses. For example, the amplitudes of peaks in the histogram presented in Fig. 1d are proportional to $\bar{P}_N^{\text{weak}}$. Therefore, the amplitude ratio of the integrated one- and two-atom peaks is $\bar{P}_2^{\text{weak}}/\bar{P}_1^{\text{weak}} = \bar{N}T/2$, which yields, based on our measurements, $\bar{N}T \approx 2.2$.

Upon strong excitation, the total signal, measured as the average number of atoms detected per laser pulse, is determined by the expression

$$S = pN_0T = \sum_{N=1}^{N_0} N\bar{P}_N^{\text{strong}} = \sum_{N=1}^{N_0} S_N. \tag{8}$$

Here, one should assume that $p = \rho_{33}$ for the spectral dependence of excitation probability. Therefore, the total signal S is in fact the result of averaging over the number of detected atoms N. The solution to the inverse problem is given by the following formula for multi-atom spectra in Fig. 3:

$$S_N = N\left(\frac{S}{N_0}\right)^N\left(1-\frac{S}{N_0}\right)^{N_0-N}\frac{N_0!}{N!(N_0-N)!}. \tag{9}$$

It follows from (9) that, in the case of mesoscopic ensembles with a small number of atoms N_0 and upon sufficiently strong excitation, a dip may arise at the centre of multi-atom resonance. This dip is caused by the pure statistical effect: the probability of exciting and detecting more than one atom is larger than the probability of exciting and detecting a single atom.

Specifically this effect is observed in Fig. 3a for the one-atom signal: there is a dip in the centre of the one-atom spectrum S_1. In the case of two atoms (spectrum S_2), there is no dip, but the resonance peak has a plateau, which is also due to the reduced probability of exciting two atoms in the resonance centre. For a larger number of atoms (multi-atom spectra), this dip is absent. A weaker dip is also observed in the one-atom spectrum in Fig. 3b at the lower three-photon Rabi frequency and, therefore, lower excitation probability. Finally, this dip completely disappears in Fig. 3c because of the insufficiently high excitation probability.

A noteworthy feature of Fig. 3 is that the widths of multi-atom resonances significantly decrease with an increase in the number of atoms N. This behaviour can be explained as follows: a one-atom spectrum is described by expression (1) or (2) for a_3, whereas upon weak excitation the N-atom spec-

trum is described by the quantity $|a_3|^{2N}(1-|a_3|^2)^{N_0-N}$, as a result of which the resonance wings are suppressed to a great extent and only its central part is retained. This circumstance was indicated for the first time by us in [3], where the possibility of applying this effect to improve the accuracy of spectroscopic measurements (if multi-atom signals from a certain number of atoms can be selectively recorded) was also discussed. For example, Eqn (1) for one atom yields a resonance width equal to Ω. In the case of N atoms, the resonance width amounts to $\Omega(2^{1/N}-1)^{1/2}$. For $N=5$, the multi-atom resonance narrows by a factor of 2.7.

The multi-atom spectra in Fig. 3 are of interest for quantum information. In particular, the dipole blockade effect can be observed in mesoscopic ensembles of cold atoms excited to Rydberg states [20, 21] if the interaction energy of Rydberg atoms exceeds the excitation resonance width (generally, the Rabi frequency). In the case of complete dipole blockade, only one atom from the entire mesoscopic ensemble can be excited to a Rydberg state, because for a larger number of atoms the collective energy levels are shifted relative to the frequency of unperturbed excitation resonance. This should lead to a radical change in the spectra presented in Fig. 3: only the one-atom signal ($N=1$) is retained, whereas all other multi-atom resonances disappear. Their incomplete disappearance may indicate incomplete dipole blockade, and the change in the resonance amplitude ratio, according to Eqn (9), allows one to determine the degree of completeness of dipole blockade under specific experimental conditions. Currently, we carry out experiments with observation of this effect upon three-photon laser excitation of Rb atoms to high Rydberg states with $n=100-120$, which are characterised by much higher interatomic interaction energies as compared with the atoms in the $37P_{3/2}$ state.

6. Conclusions

We reported the results of experimental and theoretical study of the spectra of three-photon laser excitation (according to the $5S_{1/2} \rightarrow 5P_{3/2} \rightarrow 6S_{1/2} \rightarrow 37P_{3/2}$ scheme) of mesoscopic ensembles of cold Rb Rydberg atoms in a MOT. The excitation was performed using cw single-frequency lasers in each stage. The ensembles, consisting of $N=1-5$ atoms, were detected by the SFI method, with postselection with respect to the number of atoms. The dependence of the shape of three-photon excitation spectrum on the excitation pulse duration and the number of detected Rydberg atoms was analysed.

For 2-μs pulses, the minimum spectral width amounted to 1.3 MHz; it was determined by the laser linewidths and the spectral width of laser pulses. For the pulses shorter than 0.5 μs, additional spectral broadening and occurrence of Rabi oscillations in the wings of three-photon resonances were observed, a fact suggesting that coherent three-photon laser excitation of Rydberg atoms was realised. Based on the data in the literature, we can state that this excitation was implemented for the first time. An analysis of the spectra within the four-level theoretical model based on the optical Bloch equations showed good agreement between the experiment and theory. It was concluded that, in order to increase the laser pulse coherence time, the linewidths of all laser beams should be further narrowed to 1 kHz or even less. This procedure will make it possible to observe complete Rabi oscillations upon excitation of Rydberg states and perform quantum logic gates with Rydberg atoms on their basis.

The analysis of the dependence of the shape of the three-photon excitation spectrum on the number of detected atoms showed that an increase in the average number of atoms in the one-atom excitation spectra leads to an occurrence of a dip, caused by the specificity of the excitation and detection statistics of single Rydberg atoms. The utility of multi-atom spectra is that they make it possible to reveal the presence of complete or partial dipole blockade effect for various applications of Rydberg atoms in quantum information processing. Narrowing of multi-atom spectra with an increase in the number of atoms in mesoscopic ensembles was also found. This fact can be used to improve the accuracy of spectroscopic measurements if multi-atom signals from certain numbers of atoms can be selectively detected.

Acknowledgements. This work was supported by the Russian Foundation for Basic Research [Grant Nos 16-02-00383 (in the part of theoretical analysis of laser excitation) and 17-02-00987 (in the part of applications in quantum information]; the Russian Science Foundation [Grant Nos 16-12-00028 (in the part of theoretical analysis of multi-atom signals) and 18-12-00313 (in the part of experiments on laser excitation of Rydberg atoms]; and Novosibirsk State University.

References

1. Gallagher T.F. *Rydberg Atoms* (Cambridge: Cambridge University Press, 1994).
2. Ryabtsev I.I., Tretyakov D.B., Beterov I.I., Entin V.M. *Phys. Rev. A*, **76**, 012722 (2007); Erratum: *Phys. Rev. A*, **76**, 049902(E) (2007).
3. Ryabtsev I.I., Tretyakov D.B., Beterov I.I. *J. Phys. B*, **38**, S421 (2005).
4. Saffman M., Walker T.G., Mølmer K. *Rev. Mod. Phys*., **82**, 2313 (2010).
5. Ryabtsev I.I., Beterov I.I., Tretyakov D.B., Entin V.M., Yakshina E.A. *Phys. Usp.*, **59**, 196 (2016) [*Usp. Fiz. Nauk*, **182**, 206 (2016)].
6. Saffman M. *J. Phys. B*, **49**, 202001 (2016).
7. Pohl T., Demler E., Lukin M.D. *Phys. Rev. Lett*., **104**, 043002 (2010).
8. Cinti F., Jain P., Boninsegni M., Micheli A., Zoller P., Pupillo G. *Phys. Rev. Lett*., **105**, 135301 (2010).
9. Cubel T., Teo B.K., Malinovsky V.S., Guest J.R., Reinhard A., Knuffman B., Berman P.R., Raithel G. *Phys. Rev. A*, **72**, 023405 (2005).
10. Reetz-Lamour M., Deiglmayr J., Amthor T., Weidemüller M. *New J. Phys*., **10**, 045026 (2008).
11. Sautenkov V.A., Saakyan S.A., Vilshanskaya E.V., Murashkin D.A., Zelener B.B., Zelener B.V. *Laser Phys*., **26**, 115701 (2016).
12. Maller K.M., Lichtman M.T., Xia T., Sun Y., Piotrowicz M.J., Carr A.W., Isenhower L., Saffman M. *Phys. Rev. A*, **92**, 022336 (2015).
13. Camargo F., Whalen J.D., Ding R., Sadeghpour H.R., Yoshida S., Burgdorfer J., Dunning F.B., Killian T.C. *Phys. Rev. A*, **93**, 022702 (2016).
14. Ryabtsev I.I., Beterov I.I., Tretyakov D.B., Entin V.M., Yakshina E.A. *Phys. Rev. A*, **84**, 053409 (2011).
15. Entin V.M., Yakshina E.A., Tretyakov D.B., Beterov I.I., Ryabtsev I.I. *JETP*, **116** (5), 721 (2013) [*Zh. Eksp. Teor. Fiz*., **143** (5), 831 (2013)].
16. Ryabtsev I.I., Tretyakov D.B., Beterov I.I., Entin V.M. *Phys. Rev. Lett*., **104**, 073003 (2010).

17. Tretyakov D.B., Beterov I.I., Yakshina E.A., Entin V.M., Ryabtsev I.I., Cheinet P., Pillet P. *Phys. Rev. Lett*., **119**, 173402 (2017).
18. Tretyakov D.B., Beterov I.I., Entin V.M., Ryabtsev I.I., Chapovskii P.L. *JETP*, **108**, 374 (2009) [*Zh. Eksp. Teor. Fiz*., **135**, 428 (2009)].
19. Agarwal G.S. *Phys. Rev. Lett*., **37**, 1383 (1976).
20. Lukin M.D., Fleischhauer M., Cote R., Duan L.M., Jaksch D., Cirac J.I., Zoller P. *Phys. Rev. Lett*., **87**, 037901 (2001).
21. Comparat D., Pillet P. *J. Opt. Soc. Am. B*, **27**, A208 (2010).